An efficient field-circuit coupling method by a dynamic lumped parameter reduction of the FE model

F. Henrotte, E. Lange, and K. Hameyer
Institute of Electrical Machines, RWTH Aachen University, Aachen, Germany, fh@iem.rwth-aachen.de

***Abstract*—A field-circuit coupling method is presented, whose basic idea is to extract from the FE model, on basis of energy balance considerations, a temporary lumped parameter representation of the electrical machines, to be used in the circuit simulator model of the power electronic supply. The dynamic coupled model of the complete drive obtained this way can be iterated over a limited period of time, with a time step adapted to the high frequency of electronic commutations. When the temporary representation of the machine has come, or is expected to have come under a given accuracy threshold, a new FE simulation is performed in order to generate an updated set of lumped parameters, and the process is repeated. This method allows decoupling the time constants of the field problem from that of the circuit problem, which is typically one or two orders of magnitude smaller. This yields a considerable saving of computation time with a controllable, at least a posteriori, loss of accuracy. The method presented in this paper is also characterized by the fact that only known quantities of the nonlinear FE method are used in the identification process, which can therefore be done systematically and in an automated way.**

I. Introduction

THIS paper presents a method for coupling efficiently the computational time expensive 2D or 3D Finite Element (FE) model of an electrical machine with the external power electronics circuit describing the supply system.

Over the past decades various approaches have been developed to simulate such systems supplied through high frequency switching components. Numerically strongly coupled approaches, e.g. [1]- [3], ensure consistency but suffer from long simulation times. Numerically weakly coupled approaches on the other hand, e.g. [4]- [5], are able to make benefit from the difference between the time constant of the field problem and that of the power electronics circuit, which can be of several orders of magnitude. Weak coupling allows as well to work with two specialized software, with a great benefit in flexibility and reliability.

The idea of the coupling is to extract from the FE model of the machine a set of slowly varying lumped parameters (inductances, resistances, electromotive forces) that represent the machine seen from stator terminals, and to use them in the circuit equations. The field problem is thus temporarily represented in the circuit simulator equation by a small set of lumped parameters, and time-consuming finite element simulations are done only from time to time to update this set at a rate much slower than the rate of switching of the electronic components in the supply system. The overall computation time of the coupled problem is thus considerably reduced. Additional lumped parameters for machines with rotor terminals connected to an external circuit could be treated the same way. This will however not be considered in this paper.

The updating of the lumped parameters set, is done either on a regularly basis (on the 20th circuit simulator iteration for instance), or on basis of an error estimator that triggers the generation of a new set of linearized data when the error of the present set exceeds a given threshold.

The proposed model is applied to a transformer, a permanent magnet synchronous machine (PMSM) and a three phase claw-pole alternator. The simulation results are compared with measurements and with numerical results obtained with other software packages by numerically strongly coupled approaches.

II. Lumped Parameter Extraction

A. Energy Balance in Magnetodynamics

The lumped parameters that represent an electrical machine seen from its stator terminals are the phase voltages ΔU_r, the phase resistances R_r, the inductance matrix L_{rs}, and the electromotive forces E_r induced in stator windings by the rotation of the machine, $r = 1, \ldots, m$, where $m = 3$ is the number of phases. One has

$$\Delta U_r = R_r I_r + \partial_t \varphi_r \tag{1}$$

$$= R_r I_r + E_r + L_{rs} \partial_t I_s, \tag{2}$$

where φ_r is the flux linkage in phase r.

The method presented in this paper is characterized by the fact that only known quantities of the nonlinear FE method are used for the identification process, which can therefore be done systematically and in an automated way. Those FE quatities are : the FE system matrix M_{ij}, the Jacobian matrix J_{ij} which

978-1-4244-1742-1/08/$25.00

represents the 1^{st} order linearization of the the nonlinear field equations around the system state at time t, and finally the computed torque T. All lumped parameters characterizing the FE model, as it is seen by the external circuit at time t, can be systematically extracted from them.

A relation between the field state variable (the vector potential $\mathbf{a}$) and the circuit state variables (the phase fluxes φ_r) is required for making this extraction. It is obtained on basis of energy considerations. Multiplying (1) with I_r and summing over all phases gives

$$\sum_r I_r \ \partial_t \varphi_r = -\sum_r R_r I_r^2 + \sum_r I_r \Delta U_r. \tag{3}$$

This equation has a counterpart in the field domain

$$\int_\Omega \mathbf{j} \cdot \mathcal{L}_\mathbf{v}\, \mathbf{a} = -\int_\Omega \frac{\mathbf{j}^2}{\sigma} - \int_\Omega \mathbf{j} \cdot \operatorname{grad} u, \tag{4}$$

where $\mathcal{L}_\mathbf{v}\, \mathbf{a}$ denotes the material derivative of $\mathbf{a}$, i.e. a time derivative accounting for movement [6]. Equations (4) and (3) must be identifiable term by term to ensure that the energy balance in the field domain and in the lumped parameter domain are equivalent.

The principle of the identification between field and circuit variables follows now from the observation that the current density in stranded conductors can be written

$$\mathbf{j} = \sum_r I_r \mathbf{w}_r, \tag{5}$$

where the auxiliary field $\mathbf{w}_r$ can be regarded as the shape functions of the phase currents I_r. In 2D, $\mathbf{w}_r = \pm \mathbf{e}_z P_p n_r / (\sum_k S_{rk})$, with S_{rk} are the cross section areas of all the slots carrying the current of phase r, n_r the number of turns and P_p the number of parallel paths. In 3D, $\mathbf{w}_r$ is a vector field whose field lines follow the threads of the stranded coil, Fig. 1. This vector field can be computed beforehand by an electric vector potential formulation, $\operatorname{rot} \mathbf{t} = \mathbf{j}$.

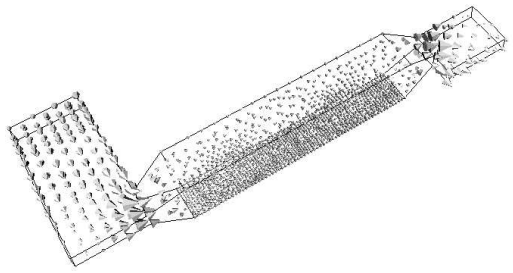

Figure 1. Current shape function of a single stator phase.

Substituting (5) in (4) yields readily

$$R_r = \int_\Omega \sigma^{-1} |\mathbf{w}_r|^2 \quad , \quad \Delta U_r = -\int_\Omega \mathbf{w}_r \cdot \operatorname{grad} u. \tag{6}$$

On the other hand, substituting (5) in

$$\int_\Omega \mathbf{j} \cdot \mathcal{L}_\mathbf{v}\, \mathbf{a} = \sum_r I_r \partial_t \varphi_r. \tag{7}$$

yields

$$\partial_t \varphi_r = \int_\Omega \mathbf{w}_r \cdot \mathcal{L}_\mathbf{v}\, \mathbf{a}. \tag{8}$$

If the current distribution functions $\mathbf{w}_r$ are assumed not to depend on time (which is exactly the case in stranded coils), the sought mapping between $\mathbf{a}$ and φ_r is

$$\varphi_r = \int_\Omega \mathbf{w}_r \cdot \mathbf{a}, \tag{9}$$

which, in a mesh, can be expressed by the rectangular matrix

$$\varphi_r = W_{ri} a_i \quad \text{with} \quad W_{ri} = \int_\Omega \mathbf{w}_r \cdot \boldsymbol{\alpha}_i \tag{10}$$

where $\boldsymbol{\alpha}_i$ are the shape functions of the $\mathbf{a}$ field, and a_i the corresponding coefficients.

B. Extraction of the inductance matrix

Let

$$M_{ij}(\mathbf{a})\ a_j = b_i, \tag{11}$$

with

$$b_i = \int_\Omega \mathbf{j} \cdot \boldsymbol{\alpha}_i = I_r \int_\Omega \mathbf{w}_r \cdot \boldsymbol{\alpha}_i = I_r W_{ir}, \tag{12}$$

be the nonlinear FE equations describing the electrical machine subjected to given phase and excitation currents.

Now, let I_r^* be the phase currents at time t, and $b_i^* = I_r^* W_{ir}$ the corresponding right-hand sides. Solving (11) with $b_i \equiv b_i^*$ and a fixed rotor angular position $\delta\Theta = 0$ gives a_j^* and a first order linearization around this particular solution writes

$$M_{ij}(a_j^* + \delta a_j) = M_{ij}(a_j^*) a_j^* + J_{ij}(a_j^*) \delta a_j = b_i^* + \delta b_i \tag{13}$$

with the Jacobian matrix $J_{ij} \equiv \left(\partial_{a_j} M_{ik}(a_j^*)\right) a_k^*$. Since $M_{ij}(a_j^*) a_j^* = b_i^*$, one has

$$J_{ij}(a_j^*)\ \ \delta a_j|_{\delta\Theta=0} = \delta b_i. \tag{14}$$

One can now repeatedly solve (14) with the right-hand sides $\delta b_i = \delta I_r\, W_{ir}$ obtained by perturbating one after the other m phase currents I_r and obtain m solution vectors for $\delta a_j|_{\delta\Theta=0}$. Since (14) is linear, the magnitude of the perturbations δI_r is arbitrary. One can so define by inspection the tangent inductance matrix L_{rs}^∂ of the electrical machine seen from terminals as

$$\begin{aligned} \delta\varphi_r|_{\delta\Theta=0} &= W_{rj}\ \ \delta a_j|_{\delta\Theta=0} \\ &= W_{rj} J_{ji}^{-1}(a_j^*) W_{is}\ \delta I_s, \equiv L_{rs}^\partial\ \delta I_s \end{aligned} \tag{15}$$

with

$$L_{rs}^\partial = W_{rj} J_{ji}^{-1}(a_j^*) W_{is}. \tag{16}$$

Similarly, one can identify the secant inductance matrix L_{rs} and by solving (11) repeatedly with linearly independent phase currents I_r to obtain

$$\varphi_r = W_{rj}\ a_j = W_{rj} M_{ji}^{-1}(a_j^*) W_{is}\ I_s \equiv L_{rs}\ I_s \tag{17}$$

with

$$L_{rs} = W_{rj} M_{ji}^{-1}(a_j^*) W_{is}. \tag{18}$$

It is practical for these identifications to use a solver capable of efficiently dealing with multiple right-hand sides.

C. Extraction of the motion induced voltage

One can now complement (15) to account for the electromotive forces. One has

$$\delta\varphi_r = L_{rs}^{\partial} \delta I_s + \partial_\Theta \varphi_r\ \delta\Theta. \tag{19}$$

The direct computation of the Θ derivative requires to slightly shift the rotor, remesh, solve the FE problem, evaluate new fluxes and calculate a finite difference. In order to avoid this tedious process, one can again call on the energy principles. One has

$$\partial_\Theta \varphi_r = \partial_\Theta \partial_{I_r} \Psi_M = \partial_{I_r} \partial_\Theta \Psi_M = \partial_{I_r} T \tag{20}$$

where T is the torque and Ψ_M is the magnetic energy of the system. During the identification process described above, it is thus easy to calculate additionally the torque corresponding to the perturbed solutions $\delta a_j|_{\delta\Theta=0}$, and to evaluate the motion induced voltage

$$E_r \equiv \partial_\Theta \varphi_r\ \partial_t \Theta \tag{21}$$

of each phase as the variation of torque with the perturbation of the corresponding phase current I_r.

Beware however that, as the torque is a nonlinear function of the fields, the perturbations needs in this case be small. Because of the linearity of (14), one may scale the perturbation currents in (20) which yields:

$$\partial_\Theta \varphi_r = \frac{T(a_j^*) - T(a_j^* + \lambda \delta a_j|_{\delta\Theta=0})}{\lambda \delta I_r} \text{ with } \lambda = \kappa \frac{||a_j^*||_2}{||\delta a_j||_2}. \tag{22}$$

The scale factor is chosen between $0.01 \leq \kappa \leq 0.05$. Both the direct calculation of the Θ derivative by finite differences and the proposed energy-based approach (22) have been implemented.

III. Realization of coupling

The numerically independent solution process of the circuit and the field problem requires a time stepping scheme synchronizing the Modified Nodal Analysis (MNA) used by the circuit simulator and the FE Analysis. A basic scheme consists in holding the time step ΔT_{FE} of the FE system constant. At the beginning of the transient simulation, the initial values of the tangent inductance matrix $L_{rs}^{\partial 0}$ and the induced voltages E_r^0 are calculated by a magnetostatic FE calculation, and incorporated into the equation system of the circuit simulator. If the circuit simulator reaches $t >= t_{FE}^{k-1} + \Delta T_{FE}$, a new set of phase currents is imposed and the magnetostatic FE model is solved, yielding an updated set of lumped parameters, $L_{rs}^{\partial k}$ and E_r^k. This basic scheme is compatible with an adaptive time stepping circuit simulator. The latter can freely adapt the time step to accurately account for topological changes occuring in the circuit, caused by e.g. switching semi-conductor components.

Any circuit simulator in combination with a magnetostatic FE-solver can be used provided both packages have proper interface capabilities. In this paper, the circuit simulator *Simplorer* [7] and the in-house FE library *i*MOOSE [8] have been used. *Simplorer* provides a C-Interface, giving access to state variable information at different stages of the time stepping scheme.

For the field and circuit simulators run on different operating systems, and in order to avoid tedious and error-prone data exchange via files, a network based data exchange has been implemented. To reduce the implementation effort to a minimum while preserving maximum flexibility, the communication is based on the free implementation omniORB [9] of the CORBA standard. All communication is done via the standard network. The CORBA standard defines a platform independent interface definition language, by which remote procedure calls are made transparent to the program designer, who need thus not worry about the implementation of a complete network stack [10].

IV. Application examples

A. Transformer

The poposed method is first validated on a 2D single phase transformer model. The primary side ($n_{pri} = 900$ turns) of the transformer is fed by the voltage source $E = 325\,\mathrm{V}\cos(2\pi \cdot \frac{t}{T})$, while the secondary side ($n_{sec} = 50$ turns) is connected to the load resistance $R_L = 3\,\Omega$.

The simulation is carried out with a fixed time step $\Delta t_c = 5 \cdot 10^{-5}\,\mathrm{s}$ for the circuit simulator and different time steps Δt_{FE} for the field domain resulting in 38, 95, 356 or 670 FE time steps, for a total simulation time of $2T = 40\,\mathrm{ms}$.

For the sake of comparison, the system is also solved by applying a numerically strong coupling with the 2D transient FE solver of the *i*MOOSE package [8]. The relative errors $e_I = (I_{ref} - I)/\max(I_{ref})$ between numerically weakly and strongly coupled approaches on the primary and secondary currents are shown in Fig. 2 and Fig. 3 respectively. Both figures reveal an error accumulation over time at a rate depending on Δt_{FE}: the smaller Δt_{FE}, the smaller the rate of amplification of the error.

The ripple observed in Fig. 3 can be ascribed to the stepwise approximation of the inductances, Fig. 4. By decreasing Δt_{FE}, the variation in time of the inductances is smoothened, which yields a more accurate result.

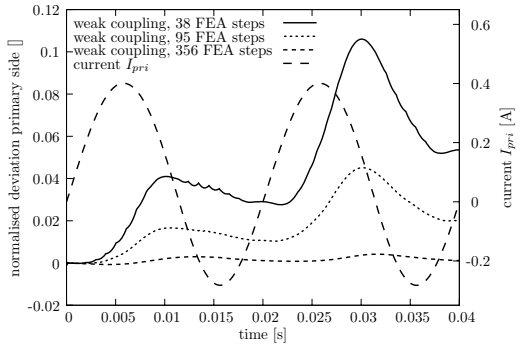

Figure 2. Relative error on the primary side current I_{pri}.

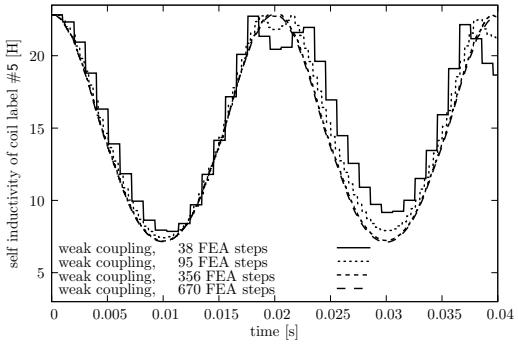

Figure 4. Linearised self inductivity of coil label #5.

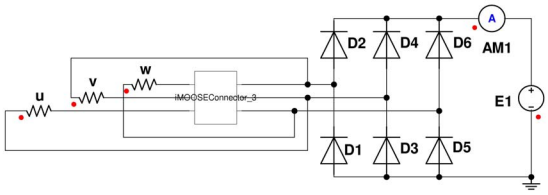

Figure 5. Generator connected to a b6 rectifier working connected to a DC voltage source.

In summary, the proposed method gives results comparables to those obtained by the strong coupling approach. Choosing an appropriate time step Δt_{FE} is however crucial to obtain accurate results.

B. Permanent Magnet Generator

The method has also been applied to a three phase synchronous permanent magnet generator connected via B6-bridge rectifier to the DC voltage source E1. The coupled problem has been simulated with both *Maxwell* [7] and the *i*MOOSE /*Simplorer* coupling described above. The topology of the system is shown in Fig. 5. The block iMOOSEConnector_3 in Fig. 5 contains the lumped parameters L_{rs}^{∂} and E_r. All circuit parameters except those lumped parameters are held constant throughout the simulation.

The comparison of the simulation results are shown in Fig. 6 and Fig. 7. The currents in phase u and the total current I_{tot} can be seen in Fig. 6. They are in good accordance, except at the beginning of the simulation. Having a closer look at the terminal voltage depicted in Fig. 7, one recognizes however overshoots at the peak values as well as around the singular switching points of the diodes in the calculation results of *Maxwell*. This behaviour indicates an inaccurate zero crossing detection in the the diodes of the bridge. The simulation results of the proposed lumped parameter coupled method are in good accordance with the simulation results of *Maxwell* with a significant time saving of approximately 25%.

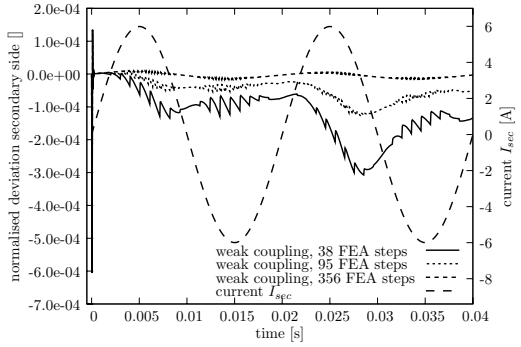

Figure 3. Relative error the secondary side current I_{sec}.

C. Claw pole generator

The proposed coupling method is finally validated on a three phase claw-pole alternator which is connected via a B6-bridge D1-D6 to the constant voltage source E1 representing the battery in series with the resistance R4, Fig. 10. Due to its irreducible 3D flux path structure and the connected bridge rectifier, the claw pole generator is a challenging field-circuit coupled system. The winding resistances are labelled R1 to R3. The excitation current is assumed to be constant in this simulation, and concerns thus only the FE system.

The inverter topology is given Fig. 10. The coupled model is simulated with the electromotive forces calculated both by finite differences and by the energy-based approach (Sec. II-C). Additionally, the software package JMAG [11] is used for the sake of comparison, see Tab. I.

The alternator is analysed at different rotation speeds. Tab. II shows the mean output currents of the alternator. Due to license issues, the simulation with JMAG at 6000 rpm could not be carried out. The simulated and measured output currents

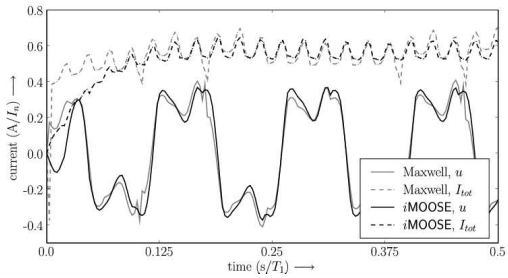

Figure 6. Total and phase u current forms at $f_1 = \frac{5}{6} T_n^{-1}$.

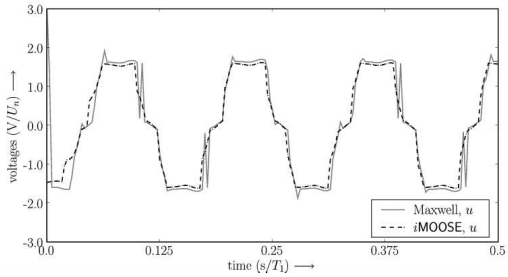

Figure 7. Terminal voltage of phase u at $f_1 = \frac{5}{6} T_n^{-1}$.

are shown in Fig. 8. While implementation a) performs well at low rotation speeds, the simulated current for the highest speed clearly exceeds the measurements. Implementation b) appears to have a small offset compared to the measurement. The implementation c) performs worst at low rotation speeds but simulates the output current very accurately at medium rotation speeds. The relative error is shown in Tab. III as well as in Fig. 9.

The induced voltages calculated by implementation a) are very sensitive to the chosen shift of the rotor. The offset of the implementation b) might stem from the calculation of the torque by the Maxwell stress tensor. A verification and comparison with different approaches of the calculation of the torque will provide useful additional information. All simulations deliver an output current larger than the measured one.

Table I
OVERVIEW OF THE NUMERICAL APPROACHES CHOSEN TO SIMULATE THE CLAW POLE ALTERNATOR.

	Simulation approach	Comment
a)	*i*MOOSE $\partial_\Theta \varphi_r$	The induced voltages are calculated by finite differences similar to postprocessing.
b)	*i*MOOSE $\partial_{I_r} M$	The induced voltages are calculated by the variational approach as proposed in II-C.
c)	JMAG	Commercial software package. Implementation and exact approach unknown.

Table II
COMPARISON OF THE MEAN OUTPUT CURRENTS OF THE CLAW POLE ALTERNATOR AT DIFFERENT ROTOR SPEEDS.

rotation speed	measured	*i*MOOSE $\partial_\Theta \varphi_r$	*i*MOOSE $\partial_{I_r} M$	JMAG
1500 rpm	45.73 A	58.80 A	65.03 A	80.04 A
1800 rpm	79.09 A	84.30 A	97.79 A	105.78 A
3000 rpm	128.76 A	145.18 A	139.12 A	131.80 A
6000 rpm	149.01 A	194.93 A	156.95 A	n.a.

Table III
RELATIVE ERROR OF THE OUTPUT CURRENT.

rotation speed	*i*MOOSE $\partial_\Theta \varphi_r$	*i*MOOSE $\partial_{I_r} M$	JMAG
1500 rpm	29 %	42 %	75 %
1800 rpm	7 %	24 %	34 %
3000 rpm	13 %	8 %	2 %
6000 rpm	31 %	5 %	n.a.

The phase and the output current waveforms simulated by implementation b) are depicted in Fig. 11. The flux density of the modeled claws is illustrated in Fig. 12.

V. DISCUSSION

The proposed field-circuit coupling method is applicable to simulate complex problems, 2D or 3D, with or without motion. Two approaches to calculate the motion induced voltages have been implemented. Despite the good agreement obtained between simulated and measured currents, the energy based approach is numerically stable. Though the calculation of the torque is crucial for this approach, it appears to be more reliable than the calculation of the electromotive forces by finite differences. Further investigations on the calculation of the torque are expected to give more information about the offset in the simulated mean output current.

The communication between *Simplorer* and *i*MOOSE via network avoids error prone file locking mechanisms necessary for synchronizing the solution process and additionally bridges the different operating systems.

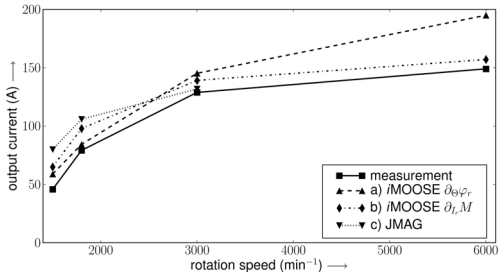

Figure 8. Comparison of the mean output currents of the claw pole alternator.

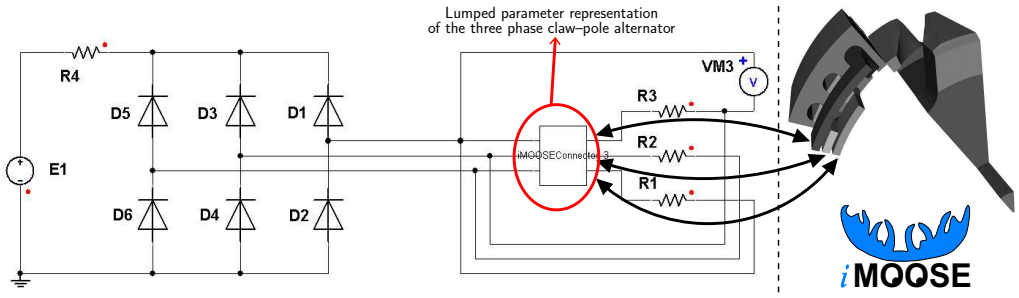

Figure 10. Application of the proposed coupling: three phase claw pole alternator connected to a rectifier working on a constant voltage source.

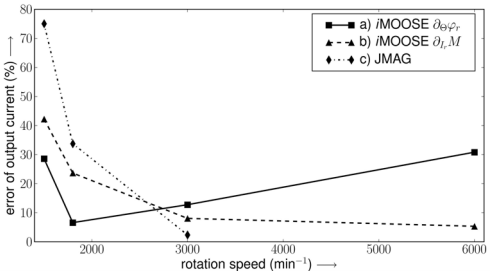

Figure 9. Relative deviation of output current through the battery E1.

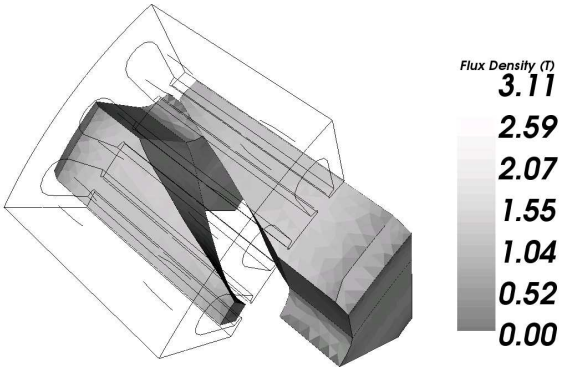

Figure 12. Midvalue of flux density at $n = 1500\,\mathrm{rpm}$ with an excitation of $I_f = 1760\,\mathrm{Aturns}$.

Furthermore, the weak coupling reduces the computation time compared to numerically strongly coupled approaches, still providing good and accurate results. During a standard simulation cycle the circuit simulator performs 10 times more transient steps before a new FE extraction is calculated. Thus, compared to numerically strongly coupled approaches, a great saving of time is achieved.

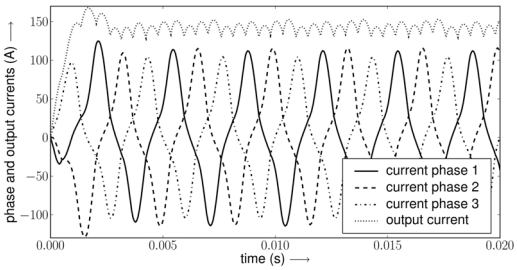

Figure 11. Phase and output current waveforms of the alternator.

REFERENCES

[1] T. Dreher, and Gérard Meunier, "3D Line Current Model of Coils and External Circuits", *IEEE Transactions on Magnetics*, vol. 31, no. 3, May 1995.

[2] P.J. Leonard, and H. C. Lai, "Treatment of Symmetry in Three Dimensional Finite Element Models of Machines Coupled to External Circuits", *IEEE Transactions on Energy Conversion*, vol. 14, no. 4, December 1999.

[3] A. Canova, M. Ottella, and D. Rodger, "Coupled Field–Circuit Approach to 3D FEM Analysis of Electromechanical Devices", *Proceedings of the 9th Int. Conf. on Electrical Machines and Drives*, pp. 71–75, 1999.

[4] P. Zhou, W. N. Fu, D. Lin, S. Stanton, and Z. J. Cendes, "Numerical Modeling of Magnetic Devices", *IEEE Transactions on Magnetics*, vol. 40, pp. 1803–1809, July 2004.

[5] P. Zhou, D. Lin, W. N. Fu, B. Ionescu, and Z. J. Cendes, "A General Cosimulation Approach for Coupled Field–Circuit Problems", *IEEE Transactions on Magnetics*, vol. 42, no. 4, pp. 1051-1054, April 2006.

[6] F. Henrotte and K. Hameyer, "The Structure of EM Energy Flows in Continuous Media", *IEEE Transactions on Magnetics*, vol. 42, no. 4, pp. 903-906, April 2006.

[7] Ansoft Corporation, "Simplorer", *http://www.ansoft.com*, [online], visited on May 9th, 2008.

[8] G. Arians, T. Bauer, C. Kaehler, W. Mai, C. Monzel, D. van Riesen and C. Schlensok, "Innovative modern object–oriented solving environment – iMOOSE", *http://www.imoose.de*, [online], visited on February 14th, 2008.

[9] Duncan Grisby, Apasphere Ltd, "omniORB – a robust high performance CORBA ORB for C++ and Python", *http://omniorb.sourceforge.net*, [online], visited on July 14th, 2008.

[10] E. Lange, M. van der Giet, F. Henrotte, K. Hameyer, "Circuit coupled simulation of a claw pole alternator by a temporary linearization of the

3D-FE model", Submitted to the XVIIIth International Conference on Electrical Machines, ICEM'08, September 2008.
[11] JRI Solutions, Ltd., "JMAG", *http://www.jri.co.jp/pro-eng/jmag/e/jmg/*, [online], visited on July 11th, 2008.
[12] H. Bai, S. Pekarek, J. Tichenor, W. Eversmann, D. Buening, G. Holbrok, M. Hull, R. Krefta, and S. Shields, "Analytical Derivation of a Coupled-Circuit Model of a Claw-Pole Alternator With Concentrated Stator Windings", *IEEE Transactions on Energy Conversion*, vol. 17, no. 1, pp. 32–38, March 2002.
[13] N. A. Demerdash and T. W. Fello, "Electric Machinery Parameters and Torques by Current and Energy Perturbations from Field Computations – Part I: Theory and Formulation", *IEEE Transactions on Energy Conversion*, vol. 14, no. 4, pp. 1507–1513, December 1999.